Transparent conducting films from $NbSe_3$ nanowires

2011 Nanotechnology 22 285202

(http://iopscience.iop.org/0957-4484/22/28/285202)

Nanotechnology **22** (2011) 285202 (5pp) doi:10.1088/0957-4484/22/28/285202

Transparent conducting films from $NbSe_3$ nanowires

Sukanta De[1], Conor S Boland[1], Paul J King[1], Sophie Sorel[1], Mustafa Lotya[1], U Patel[2], Z L Xiao[2] and Jonathan N Coleman[1]

[1] School of Physics and CRANN, Trinity College Dublin, Dublin 2, Ireland
[2] Department of Physics, Northern Illinois University, DeKalb, IL 60115, USA

E-mail: colemaj@tcd.ie

Received 7 March 2011, in final form 6 May 2011
Published 31 May 2011
Online at stacks.iop.org/Nano/22/285202

Abstract

We have developed methods to disperse and partially size separate $NbSe_3$ nanowires in aqueous surfactant solutions. These dispersions can easily be formed into thin films. Optical and electrical studies show these films to display sheet resistances and transmittances ranging from (460 Ω/□, 22%) to (12 kΩ/□, 79%) depending on thickness. For thicker films, we measured the transparent conducting figure of merit to be $\sigma_{DC,B}/\sigma_{Op} = 0.32$, similar to graphene networks. Thickness measurements gave individual values of $\sigma_{Op} = 17\,800$ S m^{-1} and $\sigma_{DC,B} = 5700$ S m^{-1}. Films thinner than ~70 nm displayed reduced DC conductivity due to percolative effects.

(Some figures in this article are in colour only in the electronic version)

1. Introduction

Transparent conducting (TC) thin films, usually doped metal oxides, are important for applications from transparent electrodes to static dissipative coatings [1]. However, due to rising material costs and the brittleness of doped metal oxides in general [2], new transparent conducting materials are urgently needed. For the most demanding applications (electrodes in displays or solar cells), requirements for transmittance and sheet resistance are $T > 90\%$ and $R_s < 100$ Ω/□ [3]. However higher resistances of a few kΩ/□ coupled with transmittances above 70% are acceptable for other applications such as window defrosting or static dissipative coatings [1]. Much work has focused on TC films from nanostructured materials [4] such as graphene [5–9], carbon nanotubes [10–15] and metallic nanowires [16–19]. Films of these materials tend to be electrically stable under flexing [8, 20]. However, each of these materials displays serious problems which reduce their potential for use as TCs. Networks of graphene have consistently displayed figures of merit that are far too low for transparent electrode applications [3]. While large area monolayer graphene films can be grown from the gas phase [21], this procedure is complex and potentially costly and will be unsuited to some applications. Although carbon nanotube thin films have been heavily studied for TC applications, they have always displayed T and R_s values below the minimum industry standard of 90% and 100 Ω/□, almost certainly due to the very large inter-tube junction resistance [22]. Finally, while networks of metallic nanowires have shown great promise and large figures of merit [16], they display relatively high resistance for thin (high transparency) films. This is due to percolation effects and is caused by their relatively large diameters [23]. This means that even these metallic nanowire networks have never surpassed $T > 90\%$ and $R_s < 100$ Ω/□. In addition, such networks suffer from haze and adhesion problems. Thus, to complete the development of nanostructured TCs, either a major breakthrough on existing materials will be required or new materials will need to be explored. In fact, a whole class of promising materials remains unexplored for this application space. These are the non-elemental inorganic nanowires which include a number of conducting members such as metal chalcogenides or doped oxide nanowires [24, 25]. Thin films of such materials have never been studied as possible TCs. In this work we fabricate thin films of $NbSe_3$ nanowires [26]. We show that these are transparent and reasonably conductive, displaying properties similar to graphene networks.

2. Experimental details

Nanowires of $NbSe_3$ were synthesized through direct reaction of stoichiometric quantities of high purity (>99.99%) niobium

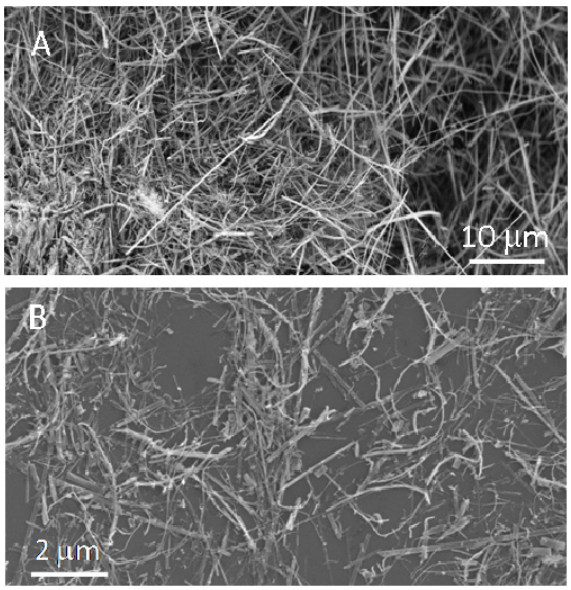

Figure 1. (A) SEM image of as-prepared $NbSe_3$ powder. (B) SEM image of a thin film of $NbSe_3$ nanowires/nanobelts prepared from a dispersion which had been centrifuged once at 500 rpm. Note the broad distribution of wire diameters and lengths.

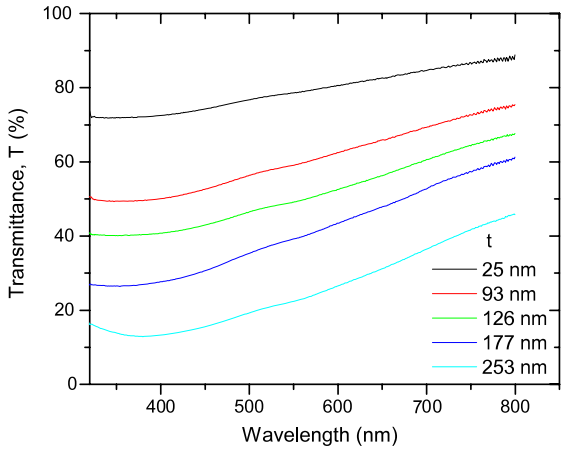

Figure 2. Transmittance spectra for films of a range of thickness' prepared from redispersed sediment after centrifugation at 3000 rpm.

and selenium powders in an evacuated quartz tube. The mixture was ground and sealed in an evacuated quartz ampoule before being heated to 700 °C at a rate of 3 °C min^{-1}, then maintained at this temperature for 1 h and cooled to room temperature at 2 °C min^{-1}. Filament-like objects, which x-ray and selected area electron diffraction analyses indicate to be monoclinic single crystalline $NbSe_3$, were found to have grown in the quartz tube (see [26] for more detail). A scanning electron microscopy (SEM) image of the as-prepared material is shown in figure 1(A). It appears to consist of a range of structural types from nanowires to nanobelts. Typically the wires/belts vary in width from tens of nanometres to ∼700 nm and can be many microns long. In some cases, the wires are aggregated in structures of ∼10 μm wide and many tens of microns long.

In order to prepare films it is necessary to first disperse the nanowires/nanobelts in the liquid phase. Following our previous work, we attempted to disperse the as-prepared material in a number of different solvents and aqueous surfactant solutions. We found that the as-prepared powder could be dispersed by sonication in isopropanol or aqueous solutions of the surfactants sodium cholate (SC) or taurodeoxycholate (TDOC). However for the isopropanol (no surfactant) dispersions, the concentrations were very low and the resultant films poor. As a result, we subsequently focused on surfactant stabilization. Typically, the dispersions were prepared by tip-sonicating (Vibra-Cell CVX; 30% × 750 W, 60 kHz) the powder (5 mg in 10 ml) for 20 min in an aqueous solution of the surfactant taurodeoxycholate (TDOC, 1 mg ml^{-1}). Depending on the exact processing procedure we found that the absorbance/cell length after a centrifugation step (500 rpm, 90 min, Hettich Mikro 22R) varied from A/l = 278 to 5.5 m^{-1}. Having estimated the absorption coefficient (550 nm) by filtration and weighing to be $\alpha \sim 5100\,Lg^{-1}\,m^{-1}$, this means the dispersed concentration varies from $C \sim 0.05$ to $\sim 10^{-3}$ mg ml^{-1} ($A/l = \alpha C$). Having tested many different procedures, the best results were found by sonicating for 20 min with a sonic tip followed by centrifugation at 500 rpm for 90 min to remove any undispersed material. The supernatant was separated from the sediment by decantation. This gave our starting stock dispersion. The stock dispersion was then deposited as a sparse network by vacuum filtration onto a porous cellulose membrane (MF-Millipore membrane, mixed cellulose esters, hydrophilic, 0.220 μm pore size, 47 mm diameter). SEM analysis (figure 1(B)) shows the dispersed nanowires to vary significantly in size and shape suggesting the need to segregate the wires by size.

Centrifugation based size separation was then performed on this stock. The stock dispersion was divided into a number of portions and each one centrifuged for 90 min at a specific rate. The rates used varied from 5000 to 500 rpm. After centrifugation, the supernatant was removed by pipette. The sediment was redispersed by addition of surfactant solution to bring it back to the original volume. This was then bath sonicated for 25 min to homogenize. Here we expect the supernatant dispersions to contain smaller nanowires/nanobelts for higher revolutions per minute (rpm). However, the redispersed sediments should contain broader size distributions of larger nanowires/nanobelts for higher rpms.

These dispersions were then filtered into films which were then transferred onto glass or plastic substrates using heat and pressure [29]. Briefly, the substrate was placed on a hot plate at 100 °C. The $NbSe_3$ nanowire film/membrane was placed on the substrate with the film in contact with the substrate. A 3 kg weight (equivalent to ∼30 kPa) was then placed on top for 2 h. The cellulose filter membrane was then removed by treatment with acetone vapour and subsequent acetone liquid baths followed by a methanol bath. We found that the best quality films were formed from TDOC dispersions. In all cases, we measured the transmittance and sheet resistance of the films. Typical transmission spectra of $NbSe_3$ films are shown in figure 2. These films typically displayed transmittance

(550 nm) between 60 and 95% and sheet resistances between 3 and 25 kΩ/□.

Transmission measurements were performed using a Varian Cary 6000i. Electrical measurements were performed using the four-probe technique with silver electrodes of dimensions and spacings typically of ∼ millimetre size and a Keithley 2400 source metre. SEM characterization was performed using a Zeiss Ultra plus SEM. Electromechanical measurements were carried out using a Zwick Z0.5 Proline tensile tester. The $NbSe_3$ nanowire film on polyethyleneterephthalate (PET) was bent into a semicircle which was constrained by the grips of the tensile tester. The film was connected via two electrodes (attached to the grips) to a Keithley KE 2601 to measure the resistance. The grip separation was then oscillated, resulting in the bending of the film between extremes characterized by bend radii of 5 and 15 mm.

3. Results and discussion

Transparent conducting materials are generally compared using figures of merit (FoM). For nanostructured transparent conductors, the FoM is often calculated using the following relationship between T and R_s [27]:

$$T = \left(1 + \frac{Z_0}{2R_s}\frac{\sigma_{Op}}{\sigma_{DC,B}}\right)^{-2} \quad (1)$$

where $Z_0 = 377\ \Omega$ is the impedance of free space and $\sigma_{DC,B}$ and σ_{Op} are the bulk DC conductivity (i.e. that of a thick film) and the optical conductivity respectively. Here $\sigma_{DC,B}/\sigma_{Op}$ can be considered a figure of merit with high values giving the required properties (high T coupled with low R_s).

Equation (1) was used to calculate $\sigma_{DC,B}/\sigma_{Op}$ from the T and R_s data for the films prepared from both sediment and supernatant as a function of centrifugation rpm (figure 3(A)). For the supernatant networks, $\sigma_{DC,B}/\sigma_{Op}$ falls steadily as the centrifugation rate increases. This indicates that the smaller objects existing in the as-prepared $NbSe_3$ powder are not suitable for use in TC networks. In contrast, for the sediment networks, $\sigma_{DC,B}/\sigma_{Op}$ increases steadily with increasing centrifugation rate before falling off at rates above 3000 rpm. This suggests that while larger (longer) wires are better, an optimum size-range exists. We examined SEM images of the networks prepared at 3000 rpm (figures 3(B) and (C)). While the networks still consist of a mixture of nanowires and nanobelts, they appear more uniform in size compared to the as-prepared material. We estimate the mean wire diameter to be ∼35 nm while the mean belt width is ∼130 nm. In a small number of cases, we observed twisted belts allowing us to estimate their thickness as ∼25 nm. The length is harder to estimate but varied from a few micron to >10 μm for both nanowires and nanobelts.

Having identified the optimum preparation conditions, we prepared a range of networks with varying thickness (controlled by the volume filtered from a dispersion of known concentration). For a particularly thick network (∼3 μm), we

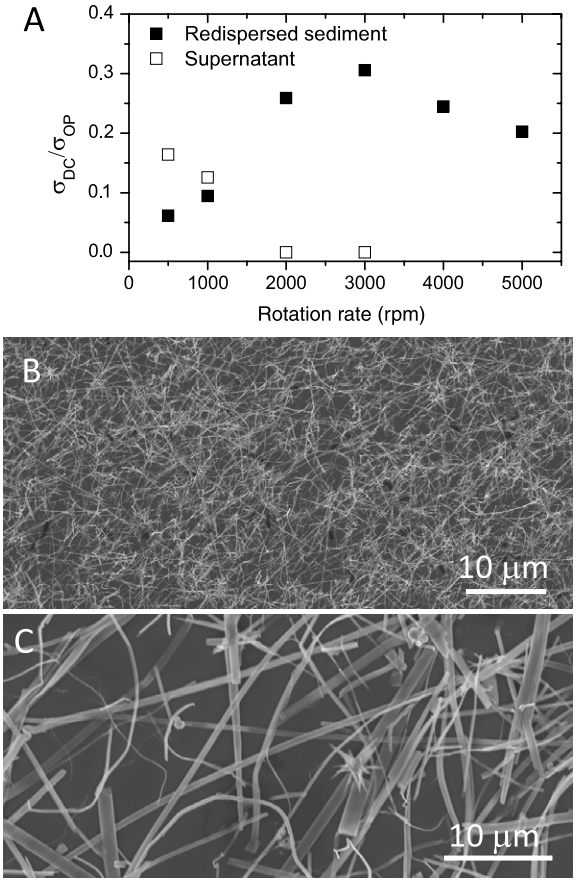

Figure 3. A) Transparent conductor figure of merit, $\sigma_{DC,B}/\sigma_{Op}$, measured for films as a function of centrifugation rate used during dispersion preparation. After centrifugation both the separated supernatant and the redispersed sediment were used to prepare films. (B) and (C) SEM images of films prepared from the redispersed sediment after centrifugation at 3000 rpm.

estimated the thickness using SEM (figure 4(A)). Knowledge of the filtered mass (from the filtered volume and dispersion concentration) then allowed the estimation of network density (∼340 kg m^{-3}) which could be used to estimate the thickness of subsequent, thinner networks. The films studied here were estimated to have mean thicknesses ranging from 25 to 250 nm. In all cases, we measured R_s and T as shown in figure 4(B). We find that decreasing the film thickness results in both R_s and T (R_s, T) increasing as expected from (460 Ω/□, 22%) to (12 k Ω/□, 79%). The portion of the graph associated with thicker films can be fitted to equation (1), giving $\sigma_{DC,B}/\sigma_{Op} = 0.32$. This value is in the range typically found for networks of graphene flakes [3].

Once the transmittance is known for a range of films of known thickness, the optical conductivity can be calculated using the expression [27]:

$$T = (1 + Z_0\sigma_{Op}t/2)^{-2}. \quad (2)$$

This is illustrated in figures 4(C) and (D) giving $\sigma_{Op} = 17\,800$ S m^{-1}, similar to carbon nanotube networks [10, 28]. Combining this with the known value of $\sigma_{DC,B}/\sigma_{Op}$, gives $\sigma_{DC,B} = 5700$ S m^{-1}. This value is comparable to that found

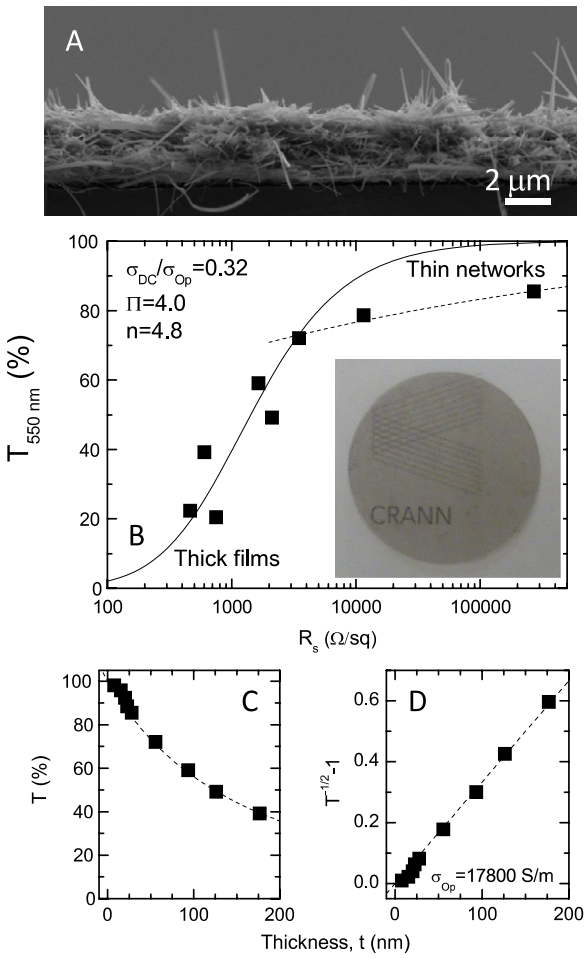

Figure 4. Analysis of films prepared from redispersed sediment after centrifugation at 3000 rpm. (A) Cross section of a thick film. (B) Plot of transmittance at 550 nm versus sheet resistance. The solid and dashed lines are fits to equations (1) and (3) respectively. Inset: Photograph of a $T = 60\%$ film. (C) Plot of transmittance at 550 nm versus film thickness. (D) The data from (C) transformed to demonstrate the agreement with equation (2). The dashed lines in (C) and (D) are fits to equation (2).

for graphene films [3] but is lower than the DC conductivity of networks of carbon nanotubes [10, 11] or silver nanowires [16]. There are two possibilities for the low conductivity, the wires themselves may be poorly conductive or the interwire junctions may be extremely resistive. Further work is required to ascertain which factor is dominant. We note that, in analogy to nanotube networks, it may be possible to improve both wire conductivity [11, 22] and junction resistance [22] by post-treatment techniques.

However, for films with thickness below ∼70 nm, the measured data deviates from the fit to equation (1). This is known to occur for thin networks of nanomaterials and is due to percolation-like effects [16, 10, 29]. Recently, we showed that, in this regime, T and R_s are described by [23]:

$$T = \left[1 + \frac{1}{\Pi}\left(\frac{Z_0}{R_s}\right)^{1/(n+1)}\right]^{-2} \tag{3}$$

where n is the percolative exponent and we denote Π as the

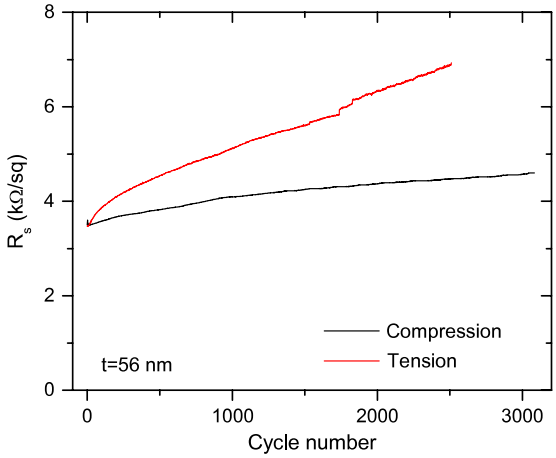

Figure 5. Electromechanical stability of $NbSe_3$ films prepared from redispersed sediment after centrifugation at 3000 rpm. We measured the sheet resistance of films transferred onto PET as the films were bent repeatedly from a radius of curvature of 15–5 mm. This was done for films on both the inside and the outside of the PET to test stability in both tension and compression. In this case, the films were 56 nm thick.

percolative FoM:

$$\Pi = 2\left[\frac{\sigma_{DC,B}/\sigma_{Op}}{(Z_0 t_{min}\sigma_{Op})^n}\right]^{1/(n+1)}. \tag{4}$$

Here, t_{min} is the critical thickness below which the DC conductivity becomes thickness dependent and which scales with the smallest dimension of nanostructured material forming the film, D, as $t_{min} \approx 2.33D$ [23]. From the intersection point of the lines in figure 4(B), we estimate $t_{min} \sim 70$ nm, consistent with the relationship above and the measured wire/belt thickness of 25–35 nm. Analysis of equations (3) and (4) shows that large values of Π but low values of n are desirable to achieve low R_s coupled with high T [23]. Fitting the data in figure 4(B) using equation (3) shows good agreement and gives the fit parameters, $\Pi = 4.0$ and $n = 4.8$. These values are inferior to those found for nanotube networks which typically display $3 < \Pi < 25$ and $0.4 < n < 1.5$ [23] but are very similar to graphene networks ($\Pi = 3.5$, $n = 3.1$) [23]. The value of Π found for these networks is low compared with nanotube networks simply because $\sigma_{DC,B}$ is low while σ_{Op}, t_{min} and n are relatively high. However, n may be high due to disorder in the network which probably leads to high junction resistances and so low $\sigma_{DC,B}$. Thus, we believe there is much scope for improvement.

Finally we tested the sheet resistance of the films as a function of bending radius, from 15 to 5 mm cycled ∼2500 times (figure 5). We found a small increase in R_s when bending in compression and a larger increase by a factor 2 when bending in tension. However, unlike indium tin oxide (ITO) [20], these films did not fail and appear relatively robust under mechanical strain. In conclusion, these materials behave similarly to graphene networks and are promising candidates for transparent conducting applications, in particular those where extremely low R_s is not required.

Acknowledgments

We acknowledge the Science Foundation Ireland funded collaboration (SFI grant 03/CE3/M406s1) between Trinity College Dublin and Hewlett Packard which has allowed this work to take place. JNC is also supported by an SFI PI award. The work on nanowire fabrication was supported by the US Department of Energy (DOE) Grant DE-FG02-06ER46334.

References

[1] Gordon R G 2000 Criteria for choosing transparent conductors *MRS Bull.* **25** 52
[2] Chen Z, Cotterell B and Wang W 2002 The fracture of brittle thin films on compliant substrates in flexible displays *Eng. Fract. Mech.* **69** 597–603
[3] De S and Coleman J N 2010 Are there fundamental limitations on the sheet resistance and transmittance of thin graphene films? *ACS Nano* **4** 2713–20
[4] Hecht D S, Hu L B and Irvin G 2011 Emerging transparent electrodes based on thin films of carbon nanotubes, graphene, and metallic nanostructures *Adv. Mater.* **23** 1482–513
[5] Becerril H A, Mao J, Liu Z, Stoltenberg R M, Bao Z and Chen Y 2008 Evaluation of solution-processed reduced graphene oxide films as transparent conductors *ACS Nano* **2** 463–70
[6] Biswas S and Drzal L T 2008 A novel approach to create a highly ordered monolayer film of graphene nanosheets at the liquidâ 'liquid interface *Nano Lett.* **9** 167–72
[7] Blake P *et al* 2008 Graphene-based liquid crystal device *Nano Lett.* **8** 1704–8
[8] De S, King P J, Lotya M, O'Neill A, Doherty E M, Hernandez Y, Duesberg G S and Coleman J N 2009 Flexible, transparent, conducting films of randomly stacked graphene from surfactant-stabilized, oxide-free graphene dispersions *Small* **6** 458
[9] Wang X, Zhi L and Mullen K 2007 Transparent, conductive graphene electrodes for dye-sensitized solar cells *Nano Lett.* **8** 323–7
[10] Doherty E M, De S, Lyons P E, Shmeliov A, Nirmalraj P N, Scardaci V, Joimel J, Blau W J, Boland J J and Coleman J N 2009 The spatial uniformity and electromechanical stability of transparent, conductive films of single walled nanotubes *Carbon* **47** 2466–73
[11] Geng H Z, Kim K K, So K P, Lee Y S, Chang Y and Lee Y H 2007 Effect of acid treatment on carbon nanotube-based flexible transparent conducting films *J. Am. Chem. Soc.* **129** 7758
[12] Hu L, Hecht D S and Gruner G 2004 Percolation in transparent and conducting carbon nanotube networks *Nano Lett.* **4** 2513–7
[13] Scardaci V, Coull R and Coleman J N 2010 Very thin transparent, conductive carbon nanotube films on flexible substrates *Appl. Phys. Lett.* **97** 023114
[14] Wu Z C *et al* 2004 Transparent, conductive carbon nanotube films *Science* **305** 1273–6
[15] Hecht D S, Heintz A M, Lee R, Hu L B, Moore B, Cucksey C and Risser S 2011 High conductivity transparent carbon nanotube films deposited from superacid *Nanotechnology* **22** 075201
[16] De S, Higgins T, Lyons P E, Doherty E M, Nirmalraj P N, Blau W J, Boland J J and Coleman J N 2009 Silver nanowire networks as flexible, transparent, conducting films: extremely high DC to optical conductivity ratios *ACS Nano* **3** 1767–74
[17] Hu L B, Kim H S, Lee J Y, Peumans P and Cui Y 2010 Scalable coating and properties of transparent, flexible, silver nanowire electrodes *ACS Nano* **4** 2955–63
[18] Lee J Y, Connor S T, Cui Y and Peumans P 2008 Solution-processed metal nanowire mesh transparent electrodes *Nano Lett.* **8** 689–92
[19] Wu H, Hu L B, Rowell M W, Kong D S, Cha J J, McDonough J R, Zhu J, Yang Y A, McGehee M D and Cui Y 2010 Electrospun metal nanofiber webs as high-performance transparent electrode *Nano Lett.* **10** 4242–8
[20] De S *et al* 2009 Transparent, flexible, and highly conductive thin films based on polymer–nanotube composites *ACS Nano* **3** 714–20
[21] Bae S *et al* 2010 Roll-to-roll production of 30 inch graphene films for transparent electrodes *Nat. Nanotechnol.* **5** 574–8
[22] Nirmalraj P N, Lyons P E, De S, Coleman J N and Boland J J 2009 Electrical connectivity in single-walled carbon nanotube networks *Nano Lett.* **9** 3890–5
[23] De S, King P J, Lyons P E, Khan U and Coleman J N 2010 Size effects and the problem with percolation in nanostructured transparent conductors *ACS Nano* **4** 7064–72
[24] Wu X C, Tao Y R, Ke X K, Zhu J M and Hong J M 2004 Catalytic synthesis of long NbS2 nanowire strands *Mater. Res. Bull.* **39** 901–8
[25] Wan Q, Dattoli E N, Fung W Y, Guo W, Chen Y B, Pan X Q and Lu W 2006 High-performance transparent conducting oxide nanowires *Nano Lett.* **6** 2909–15
[26] Hor Y S, Xiao Z L, Welp U, Ito Y, Mitchell J F, Cook R E, Kwok W K and Crabtree G W 2005 Nanowires and nanoribbons of charge–density-wave conductor NbSe3 *Nano Lett.* **5** 397–401
[27] Dressel M and Gruner G 2002 *Electrodynamics of Solids: Optical Properties of Electrons in Matter* (Cambridge: Cambridge University Press)
[28] Ruzicka B, Degiorgi L, Gaal R, Thien-Nga L, Bacsa R, Salvetat J P and Forro L 2000 Optical and dc conductivity study of potassium-doped single-walled carbon nanotube films *Phys. Rev.* B **61** R2468–71
[29] King P J, Khan U, Lotya M, De S and Coleman J N 2010 Improvement of transparent conducting nanotube films by addition of small quantities of graphene *ACS Nano* **4** 4238–46